Applied Clay Science 101 (2014) 541–552

Contents lists available at ScienceDirect

Applied Clay Science

journal homepage: www.elsevier.com/locate/clay

Research paper

Electric–hydraulic–chemical coupled modeling of solute transport through landfill clay liners

Zhenze Li [a,*], Qiang Xue [a], Takeshi Katsumi [b], Toru Inui [b]

[a] Wuhan Institute of Rock and Soil Mechanics, China Academy of Science, Wuhan, China
[b] GSGES, Kyoto University, Japan

ARTICLE INFO

Article history:
Received 12 April 2014
Received in revised form 12 September 2014
Accepted 16 September 2014
Available online 7 October 2014

Keywords:
Model
Membrane property
Osmosis
Solute transport
Liners

ABSTRACT

Pollutant migration in dense clay barriers appears to be strongly influenced by the electric double layer of colloidal surfaces. Osmosis that resulted from chemical potential or electric potential difference across the clay membrane has been successively described in a number of theoretical works. Streaming potential (SP) which is present in charged porous medium under hydraulic gradient has been recognized as a significant factor governing the mass migration in compacted clays. However, few studies have been carried out in geo-environmental area with regard to this physical phenomenon. A coupled model was proposed to account for the effects of electrical, chemical and fluidic fields on solute transport in porous medium in this study. The electrical field deals with both the streaming potential and the externally applied electrical potential. The coupled nonlinear partial differential equations are numerically simulated by finite element method. Both the steady state solution and the time-dependent solution were investigated with the consideration of a series of influential factors. The streaming potential coefficient and the electro-osmotic coefficient were found to control the solute transport process. The potential application of the materials with tendency of producing SP was discussed. With appropriate selection of materials and parameters, optimum barring effect could be obtained for soil barriers in waste containment applications.

1. Introduction

Solute transport in porous media takes place in many aspects, e.g. the engineering facilities, industrial plants and the environmental processes. In geo-environmental areas, pollutants from contaminated soils or landfills always spread towards the surroundings in terms of diffusion or advection and dispersion (Lake and Rowe, 2000; Leij et al., 1991; Rowe et al., 2000). A well designed and carefully installed barrier system for landfills usually consists of a certain number of layers of geosynthetic clay liners and compacted clay liners. The performance of these barriers is largely dependent on the capacity to resist the breakthrough of the contained pollutants. Many efforts have been made to investigate the solute transportation in dense clay liners, i.e. experimental works on parameterizations (Gorenflo et al., 2002; Manassero and Dominijanni, 2003; Rowe and Badv, 1996a; Rowe et al., 2000; Shackelford and Daniel, 1991a; Shackelford and Redmond, 1995) and theoretical works on risk analysis (Lake and Rowe, 2000; Rowe and Badv, 1996a; Rowe et al., 2000). For GCLs and compacted clays, diffusion was reported to be the dominant pattern of transport that involves a variety of solute types (Rowe and Badv, 1996a,b; Shackelford and Daniel, 1991a,b; Shackelford and Redmond, 1995). Recent studies have successfully incorporated osmosis in some solute transport models (Malusis and Shackelford, 2002; Manassero and Dominijanni, 2003; Neuzil, 2000; Olsen, 1969; Yeung and Mitchell, 1993). Yeung and Mitchell developed a coupled model to account for the chemical, hydraulic and electrical factors (Yeung and Mitchell, 1993). Manassero and Dominijanni proposed a solid theoretical framework for chemo-osmosis (Manassero and Dominijanni, 2003). The chemo-osmotic coefficient was modified by the latter study, however, irrespective of the electrical field, to predict the total barring of solute by clay membrane in extreme conditions for a perfect membrane with reflection coefficient $\omega = 1.0$ (Manassero and Dominijanni, 2003). Solute transport in charged porous medium depends on various factors such as the electrical potential derived from the concentration gradient, the electric double layer of colloids and the hydration of dissolved solutes (Chatterji, 2004). Further downward scaling will see the rising significance of the coupling effects of these factors due to the close relationship with electric double layers of colloidal surfaces.

Clay minerals, e.g. smectite and illite, have abundant permanent surface charges, high cation exchange capacity, large interlayer space, thick double electric layer and thus appear to be active in both reactivity and hydrophilicity. The flow of charged pore fluid due to a pressure gradient at zero electric current can produce potential difference, namely

* Corresponding author. Tel.: +86 27 87199858.
E-mail addresses: lazyhero@live.cn, zzli@whrsm.ac.cn (Z. Li).

http://dx.doi.org/10.1016/j.clay.2014.09.017
0169-1317/

the streaming potential (SP), through such type of porous media enriched with charged capillary (Peeters et al., 1999). Streaming potential is a typical characteristic of selective membranes which inexclusively contain the compacted clays. The direction of the resultant streaming potential relates to the positive or negative charges of a diffuse layer on colloidal surfaces. The measurement of streaming potential has been extensively used in the characterization of surface electric properties, of which the zeta potential is one of the most commonly referred and widely demanded information (Childress and Elimelech, 1996; Deshiikan et al., 1998; Deshmukh and Childress, 2001; Elimelech et al., 1994; Huisman and Trägårdh, 1999; Werner et al., 2001). Despite these investigations, streaming potential still remains to be regarded as a tool or indicator for colloidal characterizations instead of an influencing factor for solute transport through capillary porous media.

Streaming potential has widely been observed in a number of porous media, e.g. clays, rocks, mud and oil shale, in both laboratory and field studies (Chatterji, 2004; Demir, 1988; Gairon and Swartzendruber, 1975; Heister et al., 2005, 2006; Lorne et al., 1999; Tenchov, 1992). It is noted that the conduction current that resulted from the streaming potential through a porous media is non-negligible (Szymczyk et al., 2007). The migration of charged ions is likely to be influenced as long as electrical current exists in a porous medium. Heister et al. (2005) reported an obvious effect of SP on hydraulic conductivity of bentonite. Demir (1988) found a significant reduction in the flow rate and solute concentration of chloride brine through a smectite layer, which were related to the salt infiltration and streaming potential. More and more evidences clearly indicated the non-negligible coupling effects of streaming potential on permeation and solute transport (Revil et al., 2007). In spite of well-known recognition of its existence, as indicated in Yeung's paper (Yeung, 1990), few attempts have been done to take SP into the account of modeling works.

The aim of this study is to propose an electric–hydraulic–chemical coupled solute transport model to assess the complicated interaction of the multi-fields and its impact on pollutant leakage through landfill liners. Based on previous relevant theories and experimental observations, permeation-induced SP was incorporated into the governing equations with a reasonable simplification with respect to the final equilibrium state (steady state solution). The model was first validated by fitting several sets of test data about the effect of salt concentration on hydraulic conductivity of bentonite, and was further investigated numerically by varying different sets of parameters in order to understand the transport process with a bit more depth. Critical factors dominating the solute transport were discovered and evaluated numerically, revealing potential engineering application significance. The key objective of this study is not only to provide a simulational analysis of the landfill barrier system, but also to identify the governing factors that have long been ignored.

2. Theoretical framework

Various physical field variables could result in complex coupled effects on solute transport in porous medium, as shown in Table 1.

Table 1
Field variables and the coupled effects on solute transport in porous medium (after Mitchell and Soga, 2005).

Variables	Coupled effect		
	Solvent flow	Electrical current	Solute transport
Pressure head (P)	Darcy's Law	Streaming potential/ current	Advective dispersion
Electrical potential gradient (U)	Electro-osmosis	Ohm's Law	Ionic mobility
Concentration gradient (C)	Chemo-osmosis	Diffusion potential	Fick's Law

Yeung and Mitchell (1993) have reported the detailed deduction process under non-equilibrium thermodynamic principles. Manassero and Dominijanni (2003) carried out a similar study on phenomenal modeling for chemo-osmosis. The equations proposed here are consistent with these previously established models which in most parts are founded on classical assumption, however, we focus more on the development of functions and discussions relevant to streaming potential and its effect on both solute and permeate fluxes with specific assumptions.

2.1. Governing equations

2.1.1 . Solvent flux

The electro-osmotic flow could be written as (Li et al., 2011; Shang, 1997)

$$J_e = k_e \nabla(-U) \tag{1}$$

where J_e is electro-osmotic flux, k_e is electro-osmotic coefficient, and U is electrical potential. The parameter k_e (m^2/sV), which controls the water flow rate under a unit voltage gradient, is expressed in this theoretical relationship (Mitchell and Soga, 2005): $k_e = \frac{\zeta \varepsilon n}{\eta}$, where ζ (V) is the zeta potential of solids, ε (F/m) is the permittivity of the pore fluid, n is the porosity of the porous medium and η (Ns/m^2) is the viscosity of the pore fluid. It is clear that k_e is mainly governed by the zeta potential (ζ) and porosity (n) given that the permittivity and viscosity of the pore fluid remain constant.

The gradient of chemical concentration induces osmotic pressure in the form of

$$\nabla \pi = \omega RT \nabla(-C) \tag{2}$$

where π is osmotic pressure (Pa), ω is chemo-osmotic coefficient, T is temperature (K) and C is chemical concentration (M).

The fluidic flux driven by hydraulic gradient takes the form as

$$J_p = \frac{k}{\gamma V_w}[\nabla(-P) - \omega RT \nabla(-C)] \tag{3}$$

where J_p is pressure-driven flux, k is hydraulic conductivity (m/s), P is hydraulic pressure, γ is unit weight and V_w is volume of pore fluid in the representative elementary volume. The equation for J_p is consistent in form with that of Manassero and Dominijanni (2003).

The overall flux (J_v) consists of two parts,

$$J_v = J_e + J_p \tag{4}$$

Then

$$J_v = k_e \nabla(-U) + \frac{k}{\gamma V_w}[\nabla(-P) - \omega RT \nabla(-C)] \tag{5}$$

2.1.2 . Solute flux

Solute migration in liquid phase has three forms, i.e. advective–diffusion, electro-osmosis and hydraulic dispersion according to the classification in Table 1. The overall solute flux is

$$J_s = J_{ds} + J_{es} + J_{ps} \tag{6}$$

where J_s is solute flux, J_{ds} is diffusive flux, J_{es} is electro-osmotic flux and J_{ps} is dispersive flux.

Following the deduction of Yeung (1990) this equation becomes

$$J_s = nD_e \nabla(-C) + \frac{nD_e|z|FC}{RT} \nabla(-U) + (1-\omega) C J_v \tag{7}$$

where n is porosity, D_e is effective diffusion coefficient, C is solute concentration, Z is ionic charge, F is Faraday constant, R is ideal gas constant, T is temperature and ω is chemo-osmotic coefficient.

There is controversy over the form of this equation in literatures. The chemo-osmotic coefficient ω was assumed to be related to the effective diffusion coefficient ($D_e = (1-\omega)\tau D_0$, where τ is the tortuosity factor and D_0 is the free diffusion coefficient in dilute water solution) (Manassero and Dominijanni, 2003). Although its validity is hard to be verified in compacted clays, the ideal condition of total baring effect towards solute could be modeled when $\omega = 1$. After re-interpreting some reported experimental data about the diffusion coefficients and effective porosities, Manassero and Dominijanni remarked that "it seems fairly clear that on increasing the effective solute porosity ratio an increase of the tortuosity factor occurs" and believed that the proposed expression for D_e was valid (Manassero and Dominijanni, 2003). Therefore this assumption was adopted in this study and the following equation could be obtained,

$$J_s = (1-\omega)\left[nD_e\nabla(-C) + \frac{nD_e|z|FC}{RT}\nabla(-U) + CJ_v\right] \tag{8}$$

2.1.3 . Electrical current

The total electrical current density across saturated porous medium consists of two parts: 1) electrical field induced current density and 2) hydraulic gradient induced current density associated with the migration of ions in pore fluid. Revil et al. (2007) termed these two parts as conductive current density and streaming current density, separately. The conductive current density follows Ohm's law and is proportional to the local electrical field (or electrical potential difference):

$$I_e = \kappa\nabla(-U) \tag{9}$$

where I_e is electrical current density, κ is the electrical conductivity of the porous media.

The averagely oriented movement of charged ions in porous media induces the streaming current density in the form of

$$I_c = |z|FJ_s \tag{10}$$

where I_c is the streaming current density.

Then the total current density becomes

$$I = \kappa\nabla(-U) + |z|FJ_s \tag{11}$$

Heister et al. (2005) assumed that the streaming current is governed by the diffusion process, which is written as $I_c = D|z|F\nabla C$. This formula follows that proposed by Yeung (1990) and is obviously different from our assumption. Yeung (1990) assumed that the ionic mobility and the diffusion coefficient of an ion in dilute solution could be linked by the Nernst–Einstein Equation, and accordingly deduced the fractional term for the electrical current relevant to chemical potentials in the governing equations. Our model differs from the others by considering complex influential factors on solute flux in porous medium. When neglecting the convective, chemo-osmotic and electrical effects, the solute flux J_s depends merely on diffusion and then Eq. (10) equals to Eq. (12). The new expression for streaming current also complies with those adopted by Revil et al. (2007).

2.1.4 . Soil electrical conductivity

In saturated soil, the surface conductivity and liquid phase conductivity together constitute the overall bulk electrical conductivity (Revil et al., 2007; Rhoades et al., 1976). The surface conductivity depends on the electric double layer of solid phase and can be viewed as a constant while the liquid phase conductivity depends on the salinity of the pore liquid (Corwin and Lesch, 2003; Delgado et al., 2007; Zeyad et al., 1996). Thereby $\kappa = \kappa_0 + k_1C$, where k_1 is model constant, κ_0 is surface conductivity.

The surface conductivity of colloid particles is reported to be in the form of (Jiménez et al., 2007)

$$\kappa_0 = \frac{eD^{SL}}{k_BT}\sigma^{SL} \tag{12}$$

where e is the pore ratio, D^{SL} is the effective diffusion coefficient of the ion in the stagnant layer,σ^{SL} is the total surface charge in the stagnant layer, and k_B is the Boltzmann constant, and T is the absolute temperature.

The phenomenon which causes a deficit of anion in the close vicinity of negatively charged clay surface is called anion exclusion. Various experimental evidences showed that anion exclusion causes anions to move at a faster rate than the average pore water velocity and that it enhances leaching because the anions are forced into pore center where the velocity is faster (Corapcioglu and Lingam, 1994; Gvirtzman and Gorelick, 1991). Anion exclusion was reported to affect the estimates of chloride transport in field studies (Slavich and Petterson, 1993). Large scale field test further showed that the anions travelled at about twice the velocity of tritium (Gvirtzman and Gorelick, 1991). The dispersion coefficients of anions appear to greatly exceed the values expected for molecular diffusion, approximately 30 times of that for cations. The experiments of Yeung and Mitchell (1993) also confirmed this behavior. Taking into account of anion exclusion, the soil electrical conductivity can be regarded as a constant for the steady state solution that is to be discussed in the following section.

On the other hand, a steady state or final equilibrium is reported to be achievable within a certain number of pore volumes, in terms of a simple indicator as electrical conductivity which, although fluctuates at the beginning of permeation with salt solution, could eventually reach an equal level to the influent (Shackelford et al., 2010). A number of carefully designed permeation tests about compatibility of GCL and salt solutions verified this phenomenon given a sufficient equilibration time. This observation is crucial to the following analysis of the steady state solution of the coupled model regarding the assumption that the soil electrical conductivity is considered to be homogeneous throughout the porous media.

2.1.5 . Mass balance function

In case of nonreactive solute with linear, instantaneous, and reversible adsorption, the mass balance equation for the permeating solute could be written as (Shackelford and Redmond, 1995)

$$\mathrm{Div}\, J_s = -R_d n\frac{\partial C}{\partial t} \tag{13}$$

where R_d is retardation factor for sorptive chemicals, n is effective porosity of porous medium and t is diffusion time.

2.1.6 . Continuity equations

The continuity equation for incompressible fluid is shown as

$$\mathrm{Div}\, J_v = 0 \tag{14}$$

Then, applying Eq. (14) into Eq. (5) will lead to

$$\frac{\partial^2 P}{\partial x^2} = \omega RT\frac{\partial^2 C}{\partial x^2} + \frac{\gamma k_e}{k}\frac{\partial^2 U}{\partial x^2} \tag{15}$$

2.1.7 . Continuity of electrical current

For homogenous electrically conductive material, the continuity equation could be in the following form.

$$\mathrm{Div}\, I = 0 \tag{16}$$

Then, Eq. (11) could be transformed into the following form

$$\frac{\partial}{\partial x}\left(\kappa\frac{\partial U}{\partial x}\right) = |z|F\frac{\partial J_s}{\partial x} \tag{17}$$

Taking Eq. (13) into account results in the following expression

$$\frac{1}{|z|F}\frac{\partial}{\partial x}\left(\kappa\frac{\partial U}{\partial x}\right) = -R_d n\frac{\partial C}{\partial t} \tag{18}$$

In case of constant electrical conductivity as κ, it takes the reduced form as

$$\frac{\kappa}{|z|F}\frac{\partial^2 U}{\partial x^2} = -R_d n\frac{\partial C}{\partial t} \tag{19}$$

2.1.8 . Electrical potential

The streaming potential (SP) of the porous media under hydraulic gradient is written as (Gairon and Swartzendruber, 1975; Lorne et al., 1999)

$$\nabla U_{str} = k_{str}\nabla(-P) = \frac{\varepsilon_{rs}\varepsilon_0\varsigma}{\eta k_L}\nabla(-P) \tag{20}$$

where U_{str} is streaming potential that resulted from hydraulic permeation, k_{str} is the streaming potential coefficient, ε_{rs} is relative permittivity of the liquid, ε_0 is electrical permittivity of vacuum ($\mathrm{F\cdot m^{-1}}$), η is dynamic viscosity of the liquid ($\mathrm{kg\cdot m^{-1}\cdot s^{-1}}$), ζ is zeta potential of porous medium (V) and k_L is specific conductivity of the bulk liquid ($\mathrm{S\cdot m^{-1}}$).

According to the study of Gairon and Swartzendruber (1975), the coefficient k_{str} is in the range of 0.003–0.02 V/m for bentonite when permeated with water. Heister et al. (2005) reported the experimentally observed SP across bentonite permeated with salt solution, however, they did not calculate the k_{str} in both studies (Heister et al., 2005, 2006). Based on the reported test data, the maximum k_{str} was determined at 0.0024 and 0.0032 V/m for highly compacted Boom clay and bentonite, separately in presence of NaCl solution (0.1–0.01 M across the soil slice). Even for nanofiltration membranes composed of composite polymers the average k_{str} was reported to be −0.005–0.0025 V/m by Szymczyk et al. (2007). The negative value in k_{str} indicates that the surface charge of the porous media is positive. The electrical potential gradient across the compacted clay was found to be immediately developed after the application of pressure head. But the flow-induced electrical potential gradient gradually vanished, which was attributed to the decrease in salt concentration difference and the build-up of an electrical potential due to water flow (Heister et al., 2006).

With the chemo-osmotic effect accounted, the pore pressure should be modified and thus Eq. (20) turns out to be

$$\nabla U_{str} = k_{str}[\nabla(-P) - \omega RT\nabla(-C)] \tag{21}$$

As a result the overall electrical potential becomes

$$U = U_{app} + U_{str} \tag{22}$$

where U is the total electrical potential and U_{app} is the applied electrical potential.

Combining Eqs. (7), (5) into Eq. (13) will result in the following partial differential equation for chemicals

$$\begin{aligned}\frac{R_d}{1-\omega}\frac{\partial C}{\partial t} = {} & \left(D_e - \frac{k\omega RT}{\gamma}C\right)\frac{\partial^2 C}{\partial x^2} \\ & + \frac{1}{n}\left[\left(k_e + \frac{nD_e|z|F}{RT}\right)\frac{\partial U}{\partial x} + \frac{k}{\gamma}\frac{\partial P}{\partial x}\right]\frac{\partial C}{\partial x} - \frac{k\omega RT}{n\gamma}\left(\frac{\partial C}{\partial x}\right)^2 \\ & + \frac{1}{n}\left[\left(k_e + \frac{nD_e|z|F}{RT}\right)\frac{\partial^2 U}{\partial x^2} + \frac{k}{\gamma}\frac{\partial^2 P}{\partial x^2}\right]C\end{aligned} \tag{23}$$

Finally, the governing equations for the three variables, e.g. chemical concentration (C), electrical potential (U) and pore pressure (P), are all obtained as shown in Eqs. (15), (18), and (23). If we remove the terms about electrical potential from the above equations, the coupled model could be degenerated into the form of chemo-osmotically coupled model that has been previously proposed (Manassero and Dominijanni, 2003).

2.2. Numerical analysis

Analytical solutions for diffusion equations are available for certain cases with theoretical assumptions. As to the highly nonlinear differential functions, many analytical solutions are based on special boundary/initial conditions (Leij et al., 1991). It is hard to solve analytically if the boundary condition changes (Cummings et al., 2000; Ray et al., 2008; Shackelford and Redmond, 1995). Therefore, a Finite Elemental Method was used in this study to numerically solve the highly coupled nonlinear diffusion equations. With the rapid development in scientific computing and mathematical software, it tends to become much easier and more convenient to manage such kind of numerical simulations (MathWorks, 2009). The simulation scheme used here can be found in previous studies (Li, 2009; Li et al., 2011). The sketch of the landfill clay liner systems and the boundary conditions used in the numerical analysis are shown in Fig. A1 in Appendix A.

Two scenarios were considered in this study. We first analyzed a thin layer of geosynthetic clay liner (GCL) with thickness of $L = 0.01$ m with the electrical coupling deactivated in the modeling, and further compared the modeling results with a previously established model in order for verification. The second scenario represents the field condition of a compacted clay liner (CCL) for typical municipal solid waste (MSW) landfills as widely implemented in China.

Although strict legislation on the leachate level requires a maximum of 30 cm during the management of the solid waste landfills (USEPA, 1993), it proves to be very difficult and rare to achieve this objective in China, partly due to the humid climate that with abundant precipitation contributes to most of the landfill leachate. In southern China, most of the landfills have the problem of high leachate head because of the regional wet and rainy climate. The Qizishan landfill in Suzhou was reported to have more than 15 m hydraulic head of leachate above the landfill liners (Zhang, 2007). Therefore, the leachate head in this calculation example was chosen as 5.0 m (0.5 bar) above the upper surface of the barrier system. The hydraulic head difference across the barrier could be expressed as

$$P_{app} = 0.5 + \frac{L}{\gamma} \tag{24}$$

3. Results and discussion

3.1. Validation

Fig. 1a shows the comparison of breakthrough curves (BTCs) for chemicals at outlet boundary that are obtained analytically and numerically. Using the classic advective–diffusion theory, the BTCs as noted at

different depths (0.1 L, 0.5 L and 1 L) are gradually shifted towards the inlet concentration along elapsed time. The coupled model can well represent the advective–diffusion behavior of a porous medium while neglecting the coupling factors, as confirmed by the 3 BTCs that are coincident with those predicted by advective–diffusion theory. In this simulation case, model constants were taken as $k_e = k_{str} = \omega = U_0 = 0$, i.e. the influences of chemo-osmosis and electro-osmosis are negligible, representing an advection–dispersion condition. Other parameters are shown in Table 2. The model proposed in this study got validated by regarding the coincidence between the calculated BTCs and analytical solutions. We also made efforts to validate the proposed model by comparison of deducted hydraulic conductivity equation (Eq. A6 in Appendix A) with various experimental results that were collected from the literature and further analyzed in this study. Detailed information is put in Figs. A2–A3 as supplemented at the end of this paper.

3.2. Effect of streaming potential on solute transport

Fig. 1b shows the variation of solute BTCs with SP coefficient at several depths in clay barrier ($L = 1.0$ cm). At shallow depth, i.e. section B with 10% of the whole liner, the BTCs overlap each other. At deeper sections C and D, it is found that the curves with larger SP coefficient are averagely above the others. Lake and Rowe numerically analyzed GCLs with different thicknesses and found that the thinner sample was not apparently affected by the variation in diffusion parameters (Lake and Rowe, 2000). This is in good agreement with our results. Thickness of liner poses its influence on solute migration at the far end.

The effect of SP on solute BTC was further investigated by increasing the thickness of the barrier by ten times ($L = 10.0$ cm). The calculated BTCs are shown in Fig. 1c–e. The solute BTC through the same position in the barrier is found to decline with increasing k_{str} from 0 to 0.05.

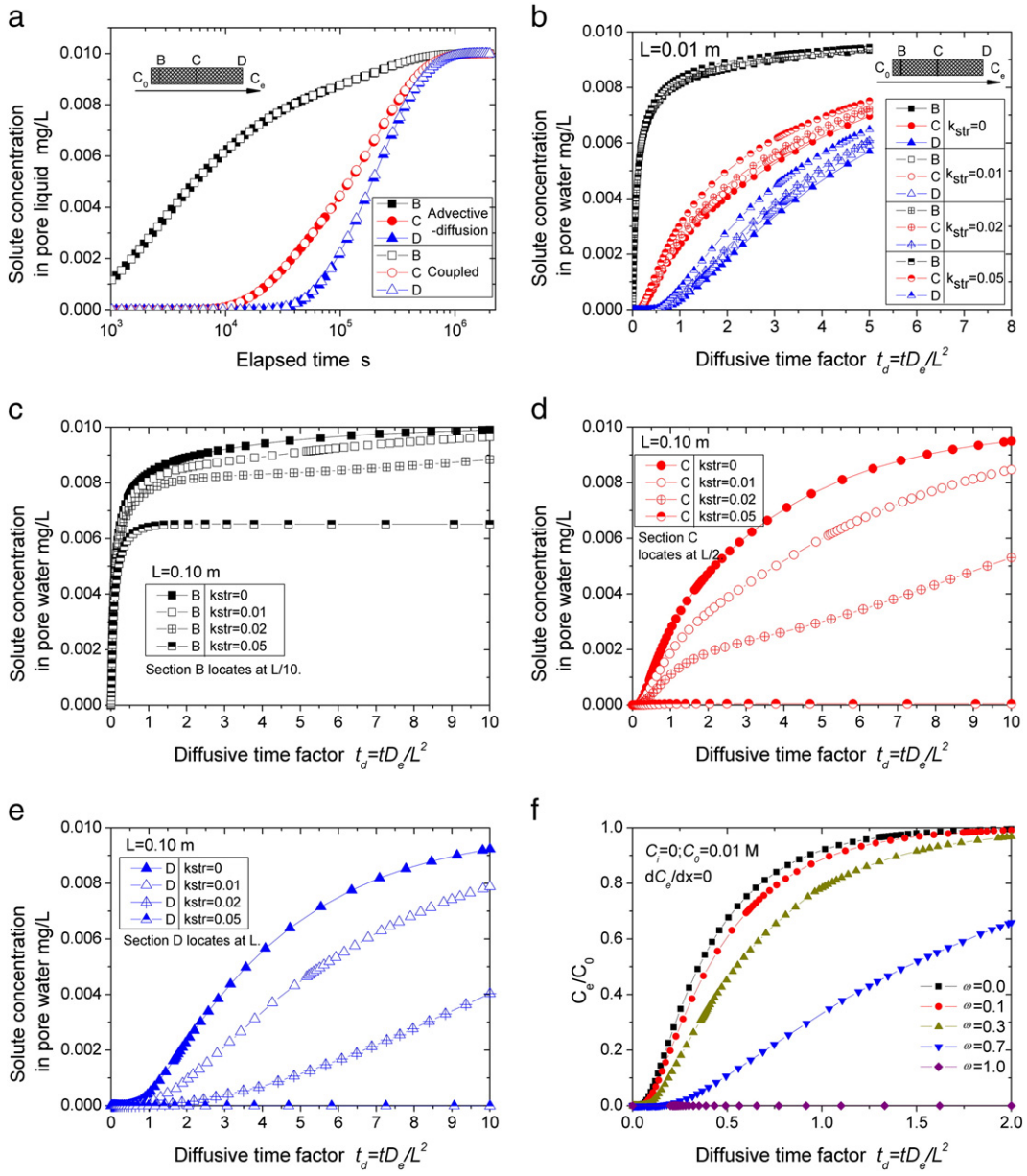

Fig. 1. Predicted breakthrough curves by FEM at various conditions. (a, BTC of different models without coupled osmosis (B: 0.1 L; C: 0.5 L; D: 1.0 L); b, variation of solute BTCs with SP constant at several depths in barrier ($i_h = 10$, $U_{app} = 0$, $\Delta C = 0.01$ M, $R_d = 10$, $L = 0.01$ m, $\kappa = 14.18C + 0.03$, $\omega = 0.1$, $k_e = 3E-8$); c, variation of solute BTCs at $L/10$ depth with SP constant k_{str} in barrier; d, BTC at $L/2$ depth; e, BTC at L depth (for c, d, and e: $i_h = 10$, $U_{app} = 0$, $\Delta C = 0.01$ M, $R_d = 10$, $L = 0.10$ m, $\kappa = 14.18C + 0.03$, $\omega = 0.1$, $k_e = 3E-8$); f, variation of solute BTCs with increasing osmotic coefficient ($i_h = 50$, $L = 0.01$ m, $\kappa = 14.18C + 0.03$, $k_{str} = 0.01$, $R_d = 1.0$, $i_U = 0$)).

Table 2
Parameters for the numerical simulation.

Symbol	Value	Unit	Notation
Basic parameters			
R	0.08206	L atm/mol K	Universal gas constant
D_e	2E−10	m^2/s	Effective diffusion coefficient
T	298	K	Temperature
ω	0.0		Osmotic efficiency coefficient
R_d	1		Retardation coefficient
γ	0.1	atm/m = 100 kN/m^3	Unit weight of water
n	0.7		Porosity
i_h	10		Hydraulic gradient
k	1E−10	m/s	Initial hydraulic conductivity
Electrical parameters			
k_e	0	m^2/V s	Electro-osmosis coefficient of soil (3E−9 (Yeung and Mitchell, 1993); 5–8E−9 for kaolin and bentonite (Yukawa et al., 1978); 5E−10–2E−9 for humidified peat (Asadi et al., 2011))
κ	0.105	S/m	Electrical conductivity of soil
Z	1		Electronic charge of the ions
F	96485.3415	s A/mol, C/mol	Faraday constant
k_{str}	0	V/atm	Constant for SP (0.3–1.7 mV/m H_2O for bentonite; 4–32 mV/m H_2O for sand–kaolin, (Gairon and Swartzendruber, 1975); 80 mV/m H_2O for crushed sandstone (Lorne et al., 1999) and 80 mV/m H_2O for kaolin in 0.001 M $CaCl_2$ observed in our study)
Size of the FEM simulation region			
L	0.01	m	Length of the FEM region
H	0.05 L	m	Width of the FEM region
$t_{\_up}$	4 L^2/D_e	s	Upper limit of transport duration
Initial conditions			
C_i	0	mol/L	Salt concentration
P_i	0	atm	Pore pressure
U_i	0	V	Applied electrical potential
Boundary conditions at inlet side			
C_0	0.01	M	Salt concentration
P_0	$i_hL/10$	atm	Pore pressure
U_0	0	V	Applied electrical potential
Boundary conditions at outlet side			
dC_e/dx	0	M/m	Dirichlet boundary
P_e	0	atm	Pressure head
U_e	0	V	Electrical potential

The maximum concentration decreases greatly from the source concentration (0.01 M) for $k_{str} = 0$ to 23.5% (2.35E−3 M) for $k_{str} = 0.05$. At section B (10% total thickness), curves with larger SP coefficient equilibrate faster. It is noteworthy that C_e at outlet (section D) drops to zero at $k_{str} = 0.05$, showing the potential of complete barring towards chemicals by the barrier in this case. We find that the overall tendency of BTCs' variation with k_{str} turns to the opposite when the barrier thickness increases from 0.01 to 0.10 m. It is supposed that interesting interactions exist between the model parameters and thickness of the barrier which will be discussed in the following parts.

3.3. Effect of chemo-osmosis on solute transport

With increasing chemo-osmotic coefficient from 0 to 1.0, the BTCs at the outlet boundary (1.0 L) shown in Fig. 1f moved to the right hand side. The time required to break through the barrier system appears to be delayed with stronger chemo-osmotic effect. Compared to similar simulation results of Manassero and Dominijanni (2003), it is observed that the BTC shown in Fig. 1f was a bit lower in location. This can be attributed to the retarding effect of streaming potential against the migration of chemicals. However, the BTC would finally approach the maximum ($C_e/C_0 = 1.0$) except for the case with total barring when $\omega = 1.0$. This is in agreement with those of Manassero and Dominijanni (2003). In the following sections, the steady state solution of our model will ignore the case of complete barring as it is few in nature.

3.4. Steady state solution

Steady state solution (SSS) relates to a special condition where all of the variables become constant regarding the time scale. Steady state physically means a final equilibrium is reached for a certain set of circumstances. It also indicates a conservative scenario and has significant implications in risk analysis of environmental assessment. Furthermore, taking SSS into account is useful for parametric analysis and has been applied to several similar studies. Manassero and Dominijanni (2003) reported the SSS of the coupling functions for the chemo-osmotic transport in porous medium. Steefel and Lasaga (1994) used SSS to investigate the validity of a numerical model that they developed to account for the coupling effects of multiple chemical species and reaction kinetics. Here we presented an evaluation of the effect of various factors on solute transport by the SSS method. This allows us to easily examine the coupling interactions of various factors and their consequences. Steady-state governing equations are expressed in the following equations:

$$\frac{\partial^2 P}{\partial x^2} + \omega RT\frac{\partial^2 C}{\partial x^2} = -\frac{1}{k_{str}}\frac{\partial^2 U_{app}}{\partial x^2} \tag{25}$$

$$\frac{\partial^2 P}{\partial x^2} - \omega RT\frac{\partial^2 C}{\partial x^2} = -\frac{1}{\frac{k}{\gamma k_e} - k_{str}}\frac{\partial^2 U_{app}}{\partial x^2} \tag{26}$$

$$nD_e\frac{\partial^2 C}{\partial x^2}+\omega RT\left[k_{str}\left(k_e+\frac{nD_e|Z|F}{RT}\right)-\frac{k}{\gamma V_w}\right]\frac{\partial}{\partial x}\left(C\frac{\partial C}{\partial x}\right)+\left[\frac{k}{\gamma V_w}-k_{str}\left(k_e+\frac{nD_e|Z|F}{RT}\right)\right]\frac{\partial}{\partial x}\left(C\frac{\partial P}{\partial x}\right)+\left(k_e+\frac{nD_e|Z|F}{RT}\right)\frac{\partial}{\partial x}\left(C\frac{\partial U_{app}}{\partial x}\right)=0 \quad (27)$$

$$1-\omega\neq 0 \quad (28)$$

The following boundary conditions were applied in the context of a landfill liner system in the following forms

$$x=0, C=C_0, U_{app}=U_0, P=P_0 \quad (29)$$

$$x=L, C=U_{app}=P=0 \quad (30)$$

The solute flux can be obtained via the SSS method. Variation of solute flux with the thickness of clay liner is shown in Fig. 2a–b. Electric potential was not present across the clay liner for these two scenarios. It is suggested that the log of solute flux decreases linearly with increasing liner thickness under the same boundary conditions. With the increase of streaming potential coefficient, the solute flux steadily decline to a considerably low level, e.g. 1E−7 mol/m^2 day at $L=0.01$ m.

Fig. 2b indicates the comparison of hydraulic boundary conditions between two cases with different k_{str}. A boundary condition with fixed value of pressure head P = 0.5 results in log(J_s)–L relationship. A more realistic form of pressure head, in terms of Eq. (24) that accounts for the impact of gravity in case of thick liner, causes a deviation from the assumed constant pressure head, particularly for thickness L > 1.0 m. The presence of streaming potential ($k_{str}=0.002$) induces a much faster reduction in solute flux at L > 1.0 m. This effect was absent and even shifted to speed up solute transport when streaming potential was nonexisting. This demonstrates the significance of streaming potential in mediation of solute flux for a clay liner.

3.4.1. Peclet number

Assuming a scenario with solely the pressure field, the Peclet number of the fluidic flow in porous media can be written as

$$P_L=\frac{k\Delta P}{n\tau\gamma D_0} \quad (31)$$

The unit of pressure P is bar, thus the specific gravity of pore liquid γ should be present in the numerator part of the fraction equation.

In this study, the electrical potential, pressure and chemical potential fields were all included. Therefore, the Peclet number should be modified to take into account of these variables.

$$P_L=\frac{k\Delta P+\gamma k_e\Delta U}{n\tau\gamma D_0} \quad (32)$$

where n is porosity, τ is the tortuosity of the pore and D_0 is the atomic diffusion coefficient in dilute solution.

Considering the following definitions,

$$\Delta P=(P_0-P_e)-\omega RT(C_0-C_e) \quad (33)$$

$$\Delta U=\Delta U_{app}+\Delta U_{str}=(U_0-U_e)-k_{str}\Delta P \quad (34)$$

and then the equation for Peclet number could be written as

$$P_L=\frac{(k/\gamma-k_ek_{str})\Delta P+k_e\Delta U_{app}}{n\tau D_0} \quad (35)$$

or

$$P_L=\frac{(k/\gamma-k_ek_{str})\Delta P_{app}-\omega RT(k/\gamma-k_ek_{str})\Delta C+k_e\Delta U_{app}}{n\tau D_0} \quad (36)$$

3.4.2. Factors affecting P_L

From Fig. 2c, the effect of osmotic coefficient on P_L was found negligible under the calculated cases. The most significant factor was the pressure head. The SP coefficient was found to affect the P_L obviously (42.8% reduction in P_L with 0.10 increase in k_{str} from 0.0), but still appeared to have less impact on P_L than the pressure head. Therefore, we conducted further calculations to investigate the effect of osmotic coefficient and pressure head on solute transport behaviors.

3.4.3. Chemo-osmotic coefficient

Fig. 2d shows the effect of chemo-osmotic coefficient on variation of solute flux at outlet with P_L. It is noted that the chemical osmosis behavior appeared to affect the solute flux at a very limited extent. The differences between the predicted curves at various osmotic coefficients were larger at $P_L<1.0$ than those at $P_L>1.0$. According to the previous study of Shackelford and Redmond, the solute transport is mainly dominated by diffusion at low Peclet No. ranges (Shackelford and Redmond, 1995). Referring to the previous analysis about the BTC of solute at various ω, the consistence of the predicted solute flux by SSS further confirmed the following principle: the presence of chemical osmosis could delay the breakthrough of the solute, but cannot decrease the flux in a long-run. Note that the outlet flux varied with P_L in a completely different way at different k_{str}. This observation is interesting and thus we made a detailed discussion as follows.

3.4.4. Effect of streaming potential coefficient on solute flux

Fig. 2e shows the variation of outlet solute flux with increasing *Peclet* number. It is interesting to find a limit state where the solute flux does not change with the *Peclet* number. In this calculation case, the *Peclet* number is mainly dependent on the applied pressure head. Referring back to the steady state equations (Eq. (28)), only the third term is relevant to P. To neglect the impact of pressure, the coefficient has to be 0. Therefore, the following relationship could be formulated:

$$k_{str}=\frac{kRT}{\gamma V_w(k_eRT+nD|Z|F)} \quad (37)$$

Based on the constants as shown in Table 2, the limit coefficient k_{str} could be determined to be 1.801E−3, which is identical to the one determined by the trial-and-error method that was used in the preparation of Fig. 2e.

As previously described, the solute BTCs for specimens with different thickness ($L=0.1$ and 0.01 m) changed with increasing SP coefficient (k_{str}) in a contradictory way. In that calculation case the pressure head gradient was fixed at 10, leading to 10 times increase in P_{app} with increasing thickness, and further giving rise to the P_L according to Eq. (31). When $k_{str}>1.801\text{E}-3$, the solute flux declines with increasing P_L, corresponding to the varying trend of BTCs as observed in those calculation examples. It is reminded that this parameter does not necessarily represent a generic situation for the membrane properties of a porous medium; instead, it is likely to be case sensitive. The declining trend of the solute flux with increasing permeate flux (equivalent to P_L) is also consistent with the experimental observations for nanofiltration (NF) membranes, as the salt rejection behavior proves to be enhanced at higher permeate fluxes by many different studies (Hagmeyer and

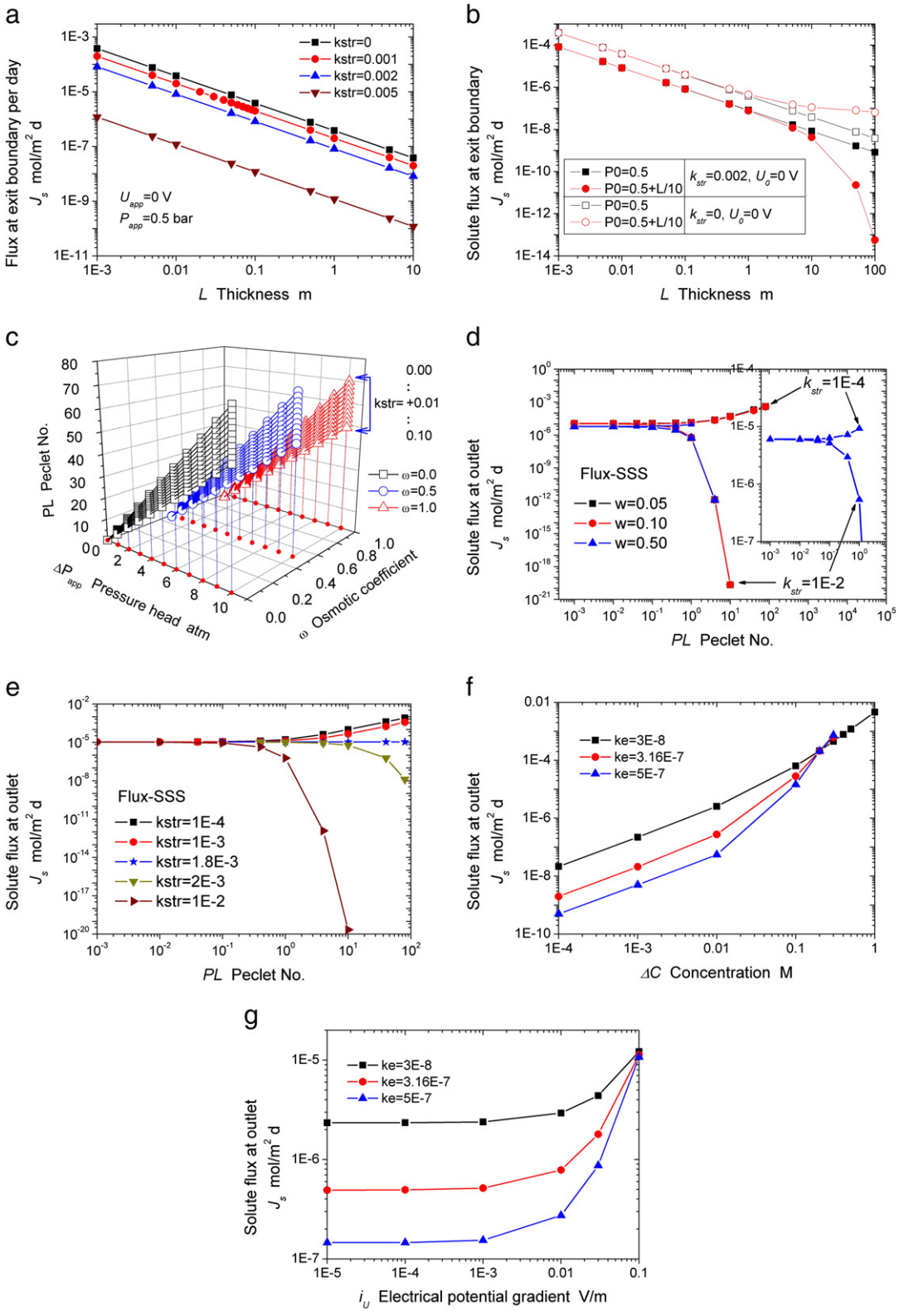

Fig. 2. Predicted solute flux at outlet of liners under various influencing factors. (a, Effect of SP constant; b, effect of pressure head; c, variation of Peclet No. under various parameter settings ($\Delta U_{app} = 0$ V; $\Delta C = 0.01$ M); d, effect of osmotic coefficient on variation of solute flux with P_L; e, effect of SP constant; f, effect of solute concentration ($L = 1.0$ m, $P_{app} = 0.5$ bar, $R_d = 1$, $k_{str} = 0.003$, $U_{app} = 0$ V); g, effect of applied electrical potential ($L = 1.0$ m, $P_{app} = 0.5$ bar, $R_d = 1$, $k_{str} = 0.003$, $\Delta C = 0.01$ M)).

Gimbel, 1998, 1999; Peeters et al., 1998, 1999; Schaep et al., 1999). Test data on microfiltration of salt solution indicates increased rejection at larger permeate flux, consistent with our models (Szymczyk et al., 2007). Experimental results show that the solute flux for the NF membrane does increase generally with increasing permeate flux despite the growing rejection rate which is defined as $R = 1 - C_e/C_0$ (Szymczyk et al., 2007). The streaming potential coefficients of these NF membranes depend on solution pH as well as salt types and concentrations. For the

conditions with the maximum salt rejection rate a higher streaming potential is always applicable to be the case. Comparatively speaking, our model demonstrates the varying tendency of solute flux for membranes permeated with different permeates under different pressure heads. Due to the fact the no information on salt rejection or solute flux is available regarding compacted clays which are the predominant type of barriers as implemented in landfills, the comparison of modeling results with NF membranes provides a supportive validation to our modeling efforts. Further experimental works about compacted clay with respect to the effect of permeate flux could be of great engineering significances.

3.4.5. Effect of solute concentration and applied electrical potential on boundary flux

Assuming a constant pressure head ($P_{app} = 0.5$ bar) upon a clay liner with $L = 0.01$ m, the effects of solute concentration and applied electrical potential on the outlet flux could be predicted by SSS as shown in Fig. 2f–g. The solute flux decreases with increasing electro-osmotic coefficient. This could be related to the SP which possesses a counter effect on solute transport. However, this behavior just validates within a certain ranges of ΔC and i_U. Critical points were observed at $\Delta C = 0.2$ M and $i_U = 0.1$ V/m where the solute fluxes were coincident to each other, although with different k_e. Outside of these regions, the effect of SP weakens compared to other field factors.

These simulations indicate that although SP could indeed help to retard solute transport in clay barrier, its applicability has a limit. The concentration inside the landfill is better to be <0.2 M in this case. In fact landfill leachate is a mixture of organics and inorganics with high value in salinity. The sodium concentration might even be beyond 6.2 g/L while the EC exceeds 4.9 S/m (Sabahi et al., 2009). In such cases, the barrier would be expected to deteriorate rapidly. As to the incinerated solid waste, solidification by cement is always applied and the solute concentration will be greatly diminished in the leachate. Such measures would partly take advantage of the barring characters of clay minerals with respect to the benefits of streaming potential.

The calculations about the applied electrical potential (Fig. 2g) demonstrate that a threshold value of SP should be overcome at the beginning of the electrokinetic processes. A minimum of applied potential gradient at 0.1 V/m should be exceeded, otherwise the electrokinetic effect would be negligible. This behavior is in good agreement with the reported electro-osmotic studies where the increase in flow rate was less proportional to the increase in applied electrical potential gradient (Asadi et al., 2009; Srivastava and Avasthi, 1973). The model might also be applicable in the electrokinetic studies, which still needs more works to do in the future.

3.5. Discussion

Theoretically the parameter k_{str} can be related to electro-osmotic coefficient k_e in the form of $k_e = k_{str} n k_L$. Comparing the value of both parameters of k_e and k_{str} reveals that the former is 4–5 orders of magnitude less than the latter. Although bulk electrical conductivity k_L is easy to be determined in experiments, the effective porosity of a porous medium composed of hydrated colloids is technically difficult to be measured. Especially for swellable clay minerals, the diffuse layer of the particle usually overlaps with each other and thus significantly reduces its effective porosity. In this study, the electro-osmotic coefficient was assumed to be constant for a permeate at certain solute concentration. In this regard, the variation of streaming potential coefficient indicates a coupling of the variation of solute concentration with porosity. It is reported that osmotic coefficients and streaming potential coefficient are dependent on salt concentration, or solution conductivity (Revil et al., 2011). Concentrated salinity leads to shrinkage of diffuse layer and weakening of surface charges, therefore constrains the membrane properties of the permeated clay liner, which is consistent with our results. Selectivity of clay minerals towards a variety of cations and its exclusion towards anions were not explicitly addressed in this study. However, it is worth of an in-depth theoretical analysis, despite its complexity as long as a combination of different solutes is present in the permeate simultaneously. The implicit approach we used in this work obscures the clear difference between them. But this does not undermine the quality of this work with regard to the steady state solution which is focused on the equilibrium state when the significance of these factors diminishes.

The variation of solute flux with P_L in cases of different k_{str} is interesting and might be important to the development of novel barrier systems. The increase in Peclet number would increase the velocity of permeate flux and thus would result in an increased solute flux, from the traditional view point. When considering the effect of SP, the common sense becomes questionable. The increase in P_L would result in decreased solute flux. This might be critical to the engineering fields like the desalination facilities, the landfill barrier systems, the water treatment sectors etc. If we can resemble the predicted effect of SP on solute transport by developing novel materials or modification methods, it would be beneficial to various engineering implementations. Heister et al. (2005) reported the presence of SP in bentonite when permeated with NaCl solution. The permeate flux through the clay specimen was observed to increase when the two ends of the specimen were short circuited, which is in good agreement with our predictions. As the streaming potential across the clay specimen was dependent on k_{str}, larger value in k_{str} results in an increased SP, and thus a lower tendency for the permeation of pore fluid. The experiments of Heister et al. (2005) further confirmed the direct relationship between the decrease of the solution flux and the gradual decline in SP with elapsed time. The quality of the barrier would be weakened with elapsed time due to the lost of the concentration difference across the barrier (Heister et al., 2005) or the lost of effective surface charges. Searching for those materials with chemo-osmotic properties has been a main purpose for membrane researchers. It is therefore expected that materials with high tendency to produce streaming potentials would greatly benefit the performance of soil barriers.

4. Conclusions

The results of this study can be summed up into the following conclusions:

A new model was proposed to account for the coupling effects of electrical, chemical and hydraulic factors on solute transport in porous media. The proposed model was verified regarding the degenerated form of equations through comparison with a previous theoretical work. Various influencing factors were investigated in terms of either the steady state solution or the time-dependent solution of the proposed theory. Membrane properties (k_{str}, k_e) were found to be the predominant factors that contribute most to the solute transport behaviors in clay liners according to the numerical simulations. The coupling of streaming potential and osmotic flow was found to impact both the hydraulic conductivity of and solute flux through the porous media. The potential application of clay minerals with varied membrane properties was further discussed with respect to the implication for the deigning of landfill clay liners, of which the optimum barrier performance could be obtained with proper selection of material and parameter.

Acknowledgment

This study was originally funded by JSPS Postdoctoral Fellowship as conducted at GSGES in Kyoto University, and subsequently revisited, continuously expanded in contents and generously supported with research grants (the China Academy of Science Interdisciplinary and Cooperative Innovation Research Team Project, NSFC grants (51279199, 51379203 and 51479194)) while the first author stayed at CAS.

Appendix A

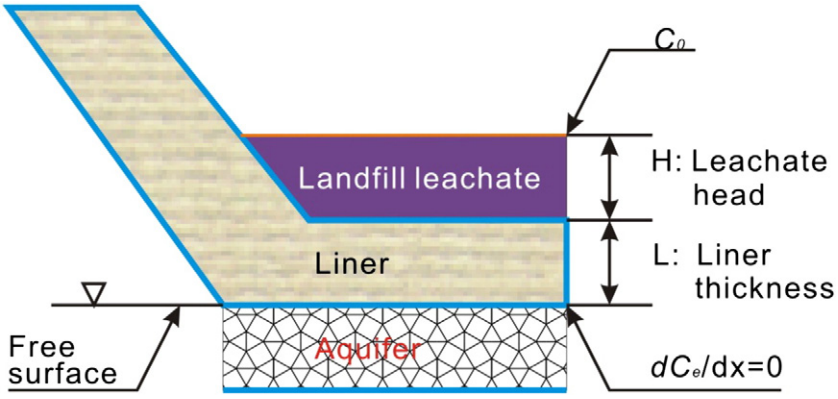

Fig. A1. Sketch of landfill liner systems and the boundary conditions used in the numerical analysis.

Validation of the proposed model with respect to permeability

Comparing the proposed model with the traditional model for solute flux in the following form

$$J_s = nD_e^0\nabla(-C) + CJ_v^0 \tag{A1}$$

leads to a new definition for hydraulic conductivity,

$$J_v^0 = k_{str}\left[\frac{nD_e zF}{RT} + (1-\omega)\left(k_e + \frac{k}{\gamma V_w}\right)\right]\nabla(-P) \tag{A2}$$

where $D_e{}^0$ is the effective diffusion coefficient without osmotic effect; $J_v{}^0$ is the permeate flux in compliance with the classical Darcy's law.

Taking account of the Darcy's law, the permeate flux becomes

$$J_v^0 = \frac{k^0}{\gamma V_w}\nabla(-P) \tag{A3}$$

where k_0 is the apparent hydraulic conductivity of the porous medium.

As

$$J_v^0 = J_v \tag{A4}$$

then

$$k^0 = k(1-\omega) - \gamma V_w k_{str}\left[\frac{nD_e zF}{RT} + (1-\omega)k_e\right] \tag{A5}$$

which can further be written as

$$k^0 = k(1-\omega) - \gamma V_w \frac{\varepsilon\zeta}{\eta k_L}\left[\frac{nD_e zF}{RT} + (1-\omega)\frac{n\varepsilon\zeta}{\eta}\right] \tag{A6}$$

The above equation can be symbolized into the following equation

$$k^0 = \alpha + \beta\zeta + \chi\zeta^2 \tag{A7}$$

where the three model constants read as

$$\alpha = k(1-\omega) \tag{A8}$$

$$\beta = -\gamma V_w \frac{\varepsilon nD_e zF}{\eta k_L RT} \tag{A9}$$

$$\chi = -(1-\omega)\gamma V_w \frac{n\varepsilon^2}{k_L\eta^2} \tag{A10}$$

When neglecting chemo-osmotic effect and the variation of permittivity of pore fluid, these three coefficients can be viewed as constants. A polynomial equation (Eq. (A7)) holds true within a certain range of zeta potentials for a specific clay mineral.

Aydin et al. investigated the dependence of zeta potential and permeability of compacted clay on cationic sorption and solution properties, based on which an exponential relationship was found between k and ζ (Aydin et al., 2004). But we also found that a polynomial equation can best-fit the experimental results with high correlation coefficient, which supports our proposed model. Lee et al. (2005) investigated the relationship between various index properties and hydraulic conductivity for bentonite and their results are shown in Fig. A2. The discrepancy between these two series of data is due to the difference in the dry densities of specimens.

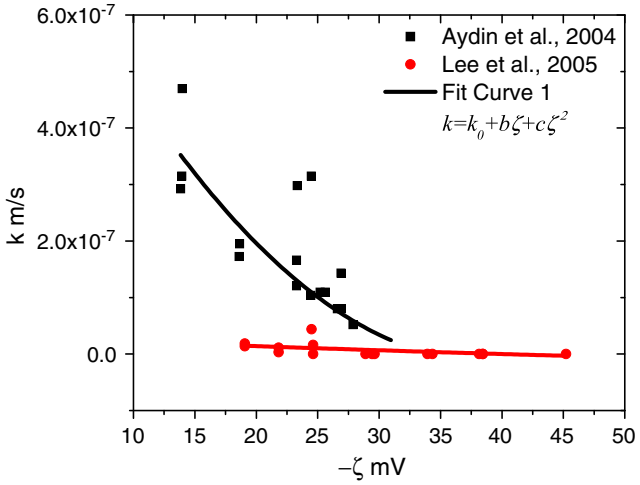

Fig. A2. Variation of hydraulic conductivity with zeta potential of clay minerals (both for bentonite with different porosities).

Experiments show that zeta potential of clay minerals vary with pH and divalent cationic concentrations in an exponential way (Baik and Lee, 2010; Niriella and Carnahan, 2006). Bentonite was reported to have negative zeta potentials at a wide range of solution pHs 2–12 (Baik and Lee, 2010; Yoshida and Suzuki, 2008). Katsumi et al. developed a new type of organo-bentonite by surfactant intercalation

and found that it is particularly resistant to chemical attack, as shown in Fig. A3. A uniform and stable ζ can be expected for this material. Taking these features into account, the ζ can be modeled by

$$\zeta = A\exp(-BC) \tag{A11}$$

where A and B are model constants, C is solute concentration in pore fluid. Accordingly, a polynomial equation with exponential terms can be applied to fit the relationship between k and C as shown in Fig. A3.

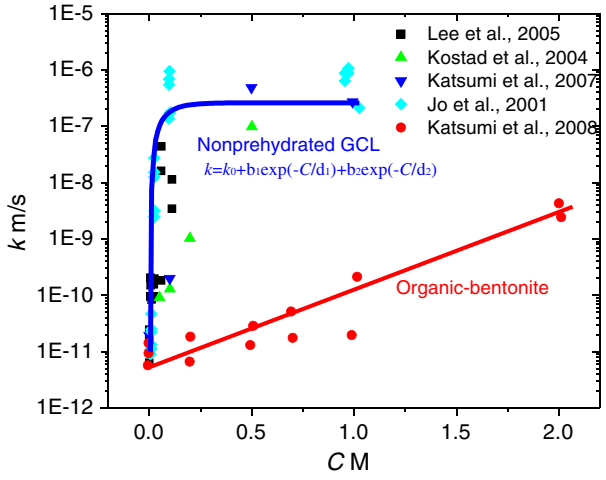

Fig. A3. Variation of hydraulic conductivity with solute concentration (the permeate used in these tests were all divalent cations).

Steady state solution and its comparison with time-dependent cumulative solution

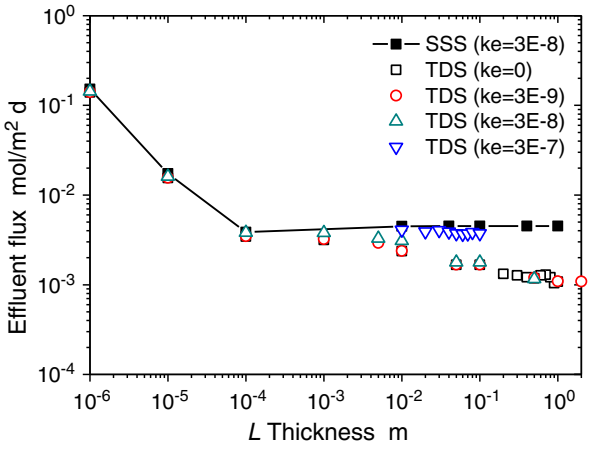

Fig. A4. Difference between time-dependent solution and steady state solution ($i_U = 10$ V/m, $i_h = 50$, $\kappa = 14.18C + 0.03$, $\omega = 0.1$, $R_d = 1$, $k_{str} = 0.01$, $D_e = 2E-10$, $k = 1E-10$).

Fig. A4 shows the difference between the determined solute flux at the outlet boundary by different method, steady state solution (SSS) and time-dependent solution (TDS). When calculated by the finite element method, the precision of TDS seems not satisfying compared to that of SSS. All of the TDS appeared to be conservative since the values were less than the relevant SSS, with an average difference at 13.3%. The authors attempted to calculate the numerical solutions for barriers at varying thicknesses from 0.001 to 1.0 m, the SSS succeeds at most of these range, but the TDS fails in most cases except those shown in Fig. A4. The CPU time required to obtain the TDS was much larger than that for SSS. Therefore, the following discussions were conducted mainly concerning the SSS.

The Peclet number P_L could be determined to be 1875.0 (L = 1.0 m) according to Eq. (35). This might be able to explain the observation of strange varying pattern of flux with the barrier thickness. It is believed that the advection–diffusion transport model could not fit very well the situations with very high Peclet column number (Brady and Morris, 1997; Calhoun and LeVeque, 2000; Giona et al., 2004; Heyes and Melrose, 1993; Morris and Brady, 1996). From a microscale perspective, strong shear between the constituent of the pore liquid was yielded in high P_L cases. The effects of Brownian motion of solute and the interparticle force of hard-sphere type fluid upon the particle configuration should be analyzed (Brady and Morris, 1997). Novel algorithm for advection–diffusion equations in both irregular geometries and high P_L situations (Calhoun and LeVeque, 2000), which is out of the scope of the current study, should be further accounted to solve the potential numerical difficulties.

References

Asadi, A., Huat, B.B.K., Hassim, M.M., 2009. Electroosmotic phenomena in organic soils. Am. J. Environ. Sci. 5, 310–314.

Asadi, A., Huat, B.B.K., Moayedi, H., Shariatmadari, N., Parsaie, A., 2011. Electro-osmotic permeability coefficient of peat with different degree of humification. Int. J. Electrochem. Sci. 6, 4481–4492.

Aydin, M., Yano, T., Kilic, S., 2004. Dependence of zeta potential and soil hydraulic conductivity on adsorbed cation and aqueous phase properties. Soil Sci. Soc. Am. J. 68, 450–459.

Baik, M.H., Lee, S.Y., 2010. Colloidal stability of bentonite clay considering surface charge properties as a function of pH and ionic strength. J. Ind. Eng. Chem. 16, 837–841.

Brady, J.F., Morris, J.F., 1997. Microstructure of strongly sheared suspensions and its impact on rheology and diffusion. J. Fluid Mech. 348, 103–139.

Calhoun, D., LeVeque, R.J., 2000. A Cartesian grid finite-volume method for the advection–diffusion equation in irregular geometries. J. Comput. Phys. 157, 143–180.

Chatterji, S., 2004. Ionic diffusion through thick matrices of charged particles. J. Colloid Interface Sci. 269, 186–191.

Childress, A.E., Elimelech, M., 1996. Effect of solution chemistry on the surface charge of polymeric reverse osmosis and nanofiltration membranes. J. Membr. Sci. 119, 253–268.

Corapcioglu, M.Y., Lingam, R., 1994. The anion exclusion phenomenon in the porous media flow: a review. In: Corapcioglu, M.Y. (Ed.), Advances in Porous Media. Elsevier Science Publishers, Amsterdam.

Corwin, D.L., Lesch, S.M., 2003. Application of soil electrical conductivity to precision agriculture: theory, principles, and guidelines. Agron. J. 95, 455–471.

Cummings, E.B., Griffiths, S.K., Nilson, R.H., Paul, P.H., 2000. Conditions for similitude between the fluid velocity and electric field in electroosmotic flow. Anal. Chem. 72, 2526–2532.

Delgado, A.V., Gonzanez-Caballero, F., Hunter, R.J., Koopal, L.K., Lyklema, J., 2007. Measurement and interpretation of electrokinetic phenomena. J. Colloid Interface Sci. 309, 194–224.

Demir, I., 1988. The interrelation of hydraulic and electrical conductivities, streaming potential, and salt filtration during the flow of chloride brines through a smectite layer at elevated pressures. J. Hydrol. 98, 31–52.

Deshiikan, S.R., Eschenazi, E., Papadopoulos, K.D., 1998. Transport of colloids through porous beds in the presence of natural organic matter. Colloids Surf. A Physicochem. Eng. Asp. 145, 93–100.

Deshmukh, S.S., Childress, A.E., 2001. Zeta potential of commercial RO membranes: influence of source water type and chemistry. Desalination 140, 87–95.

Elimelech, M., Chen, W.H., Waypa, J.J., 1994. Measuring the zeta (electrokinetic) potential of reverse osmosis membranes by a streaming potential analyzer. Desalination 95, 269–286.

Gairon, S., Swartzendruber, D., 1975. Water flux and electrical potentials in water-saturated bentonite. Soil Sci. Soc. Am. J. 39, 811–817.

Giona, M., Cerbelli, S., Vitacolonna, V., 2004. Universality and imaginary potentials in advection–diffusion equations in closed flows. J. Fluid Mech. 513, 221–237.

Gorenflo, R., Mainardi, F., Moretti, D., Pagnini, G., Paradisi, P., 2002. Discrete random walk models for space–time fractional diffusion. Chem. Phys. 284, 521–541.

Gvirtzman, H., Gorelick, S.M., 1991. Dispersion and advection in unsaturated porous-media enhanced by anion exclusion. Nature 352, 793–795.

Hagmeyer, G., Gimbel, R., 1998. Modelling the salt rejection of nanofiltration membranes for ternary ion mixtures and for single salts at different pH values. Desalination 117, 247–256.

Hagmeyer, G., Gimbel, R., 1999. Modelling the rejection of nanofiltration membranes using zeta potential measurements. Sep. Purif. Technol. 15, 19–30.

Heister, K., Kleingeld, P.J., Gustav Loch, J.P., 2005. Quantifying the effect of membrane potential in chemical osmosis across bentonite membranes by virtual short-circuiting. J. Colloid Interface Sci. 286, 294–302.

Heister, K., Kleingeld, P.J., Loch, J.P.G., 2006. Induced membrane potentials in chemical osmosis across clay membranes. Geoderma 136, 1–10.

Heyes, D.M., Melrose, J.R., 1993. Brownian dynamics simulations of model hard-sphere suspensions. J. Non-Newtonian Fluid Mech. 46, 1–28.
Huisman, I.H., Trägårdh, G., 1999. Determining the zeta potential of ultrafiltration membranes using their salt retention. Colloids Surf. A Physicochem. Eng. Asp. 157, 261–268.
Jiménez, M.L., Arroyo, F.J., Carrique, F., Delgado, A.V., 2007. Surface conductivity of colloidal particles: experimental assessment of its contributions. J. Colloid Interface Sci. 316, 836–843.
Lake, C.B., Rowe, R.K., 2000. Diffusion of sodium and chloride through geosynthetic clay liners. Geotext. Geomembr. 18, 103–131.
Lee, J.M., Shackelford, C.D., Benson, C.H., Jo, H.Y., Edil, T.B., 2005. Correlating index properties and hydraulic conductivity of geosynthetic clay liners. J. Geotech. Geoenviron. 131, 1319–1329.
Leij, F.J., Skaggs, T.H., Vangenuchten, M.T., 1991. Analytical solutions for solute transport in 3-dimensional semi-infinite porous-media. Water Resour. Res. 27, 2719–2733.
Li, Z.Z., 2009. Mechanism of Sorption, Desorption, Diffusion and Remediation of Heavy Metals Soils (in Chinese). Zhejiang University, Hangzhou, China (PhD).
Li, Z.Z., Katsumi, T., Inui, T., 2011. Modeling cake filtration under coupled hydraulic, electric and osmotic effects. J. Membr. Sci. 378, 485–494.
Lorne, B., Perrier, F., Avouac, J.P., 1999. Streaming potential measurements 2. Relationship between electrical and hydraulic flow patterns from rock samples during deformation. J. Geophys. Res. Solid Earth 104, 17879–17896.
Malusis, M.A., Shackelford, C.D., 2002. Coupling effects during steady-state solute diffusion through a semipermeable clay membrane. Environ. Sci. Technol. 36, 1312–1319.
Manassero, M., Dominijanni, A., 2003. Modelling the osmosis effect on solute migration through porous media. Geotechnique 53, 481–492.
MathWorks, 2009. MATLAB Tutorial. The MathWorks, Natick, MA, USA.
Mitchell, J.K., Soga, K., 2005. Fundamentals of Soil Behaviors. Wiley.
Morris, J.F., Brady, J.F., 1996. Self-diffusion in sheared suspensions. J. Fluid Mech. 312, 223–252.
Neuzil, C.E., 2000. Osmotic generation of 'anomalous' fluid pressures in geological environments. Nature 403, 182–184.
Niriella, D., Carnahan, R.P., 2006. Comparison study of zeta potential values of bentonite in salt solutions. J. Dispers. Sci. Technol. 27, 123–131.
Olsen, H.W., 1969. Simultaneous fluxes of liquid and charge in saturated kaolinite. Soil Sci. Soc. Am. J. 33, 338–344.
Peeters, J.M.M., Boom, J.P., Mulder, M.H.V., Strathmann, H., 1998. Retention measurements of nanofiltration membranes with electrolyte solutions. J. Membr. Sci. 145, 199–209.
Peeters, J.M.M., Mulder, M.H.V., Strathmann, H., 1999. Streaming potential measurements as a characterization method for nanofiltration membranes. Colloids Surf. A Physicochem. Eng. Asp. 150, 247–259.
Ray, S.S., Chaudhuri, K.S., Bera, R.K., 2008. Application of modified decomposition method for the analytical solution of space fractional diffusion equation. Appl. Math. Comput. 196, 294–302.
Revil, A., Linde, N., Cerepi, A., Jougnot, D., Matthai, S., Finsterle, S., 2007. Electrokinetic coupling in unsaturated porous media. J. Colloid Interface Sci. 313, 315–327.
Revil, A., Woodruff, W.F., Lu, N., 2011. Constitutive equations for coupled flows in clay materials. Water Resour. Res. 47, 1–21.
Rhoades, J.D., Raats, P.A.C., Prather, R.J., 1976. Effects of liquid-phase electrical-conductivity, water-content, and surface conductivity on bulk soil electrical-conductivity. Soil Sci. Soc. Am. J. 40, 651–655.
Rowe, R.K., Badv, K., 1996a. Chloride migration through clayey silt underlain by fine sand or silt. J. Geotech. Eng. ASCE 122, 60–68.
Rowe, R.K., Badv, K., 1996b. Advective–diffusive contaminant migration in unsaturated sand and gravel. J. Geotech. Eng. ASCE 122, 965–975.
Rowe, R.K., Lake, C.B., Petrov, R.J., 2000. Apparatus and procedures for assessing inorganic diffusion coefficients for geosynthetic clay liners. Geotech. Test. J. 23, 206–214.
Sabahi, A.E., Rahim, S.A., Wan Zuhairi, W.Y., 2009. The characteristics of leachate and groundwater pollution at municipal solid waste landfill of Ibb City, Yemen. Am. J. Environ. Sci. 5, 256–266.
Schaep, J., Vandecasteele, C., Peeters, B., Luyten, J., Dotremont, C., Roels, D., 1999. Characteristics and retention properties of a mesoporous γ-Al2O3 membrane for nanofiltration. J. Membr. Sci. 163, 229–237.
Shackelford, C.D., Daniel, D.E., 1991a. Diffusion in saturated soil. 2. Results for compacted clay. J. Geotech. Eng. ASCE 117, 485–506.
Shackelford, C.D., Daniel, D.E., 1991b. Diffusion in saturated soil. 1. Background. J. Geotech. Eng. ASCE 117, 467–484.
Shackelford, C.D., Redmond, P.L., 1995. Solute breakthrough curves for processed kaolin at low-flow rates. J. Geotech. Eng. ASCE 121, 17–32.
Shackelford, C.D., Sevick, G.W., Eykholt, G.R., 2010. Hydraulic conductivity of geosynthetic clay liners to tailings impoundment solutions. Geotext. Geomembr. 28, 149–162.
Shang, J.Q., 1997. Zeta potential and electroosmotic permeability of clay soils. Can. Geotech. J. 34, 627–631.
Slavich, P.G., Petterson, G.H., 1993. Anion exclusion effects on estimates of soil chloride and deep percolation. Aust. J. Soil Res. 31, 455–463.
Srivastava, R.C., Avasthi, P.K., 1973. Electro-osmotic effects in a bentonite–water system. J. Hydrol. 20, 37–47.
Steefel, C.I., Lasaga, A.C., 1994. A coupled model for transport of multiple chemical-species and kinetic precipitation dissolution reactions with application to reactive flow in single-phase hydrothermal systems. Am. J. Sci. 294, 529–592.
Szymczyk, A., Fatin-Rouge, N., Fievet, P., 2007. Tangential streaming potential as a tool in modeling of ion transport through nanoporous membranes. J. Colloid Interface Sci. 309, 245–252.
Tenchov, G.G., 1992. Streaming potential and SP log in shaly sands. J. Pet. Sci. Eng. 7, 309–318.
USEPA, 1993. Solid Waste Disposal Facility Criteria-Technical Manual. EPA530-R-93-017.
Werner, C., Zimmermann, R., Kratzmüller, T., 2001. Streaming potential and streaming current measurements at planar solid/liquid interfaces for simultaneous determination of zeta potential and surface conductivity. Colloids Surf. A Physicochem. Eng. Asp. 192, 205–213.
Yeung, A.T., 1990. Coupled flow equations for water, electricity and ionic contaminants through clayey soils under hydraulic, electrical and chemical gradients. J. Non-Equilib. Thermodyn. 15, 247–267.
Yeung, A.T., Mitchell, J.K., 1993. Coupled fluid, electrical and chemical flows in soil. Geotechnique 43, 121–134.
Yoshida, T., Suzuki, M., 2008. Effects of humic acid on migration of montmorillonite and alumina colloid in a quartz sand column. Colloids Surf. A Physicochem. Eng. Asp. 325, 115–119.
Yukawa, H., Yoshida, H., Kobayashi, K., Hakoda, M., 1978. Electroosmotic dewatering of sludge under condition of constant voltage. J. Chem. Eng. Jpn 11, 475–480.
Zeyad, S.A., Craig, H.B., Lisa, R.B., 1996. Electrical resistivity of compacted clays. J. Geotech. Eng. ASCE 122, 397–406.
Zhang, W.J., 2007. Experimental and numerical study on water/leachate transport in landfill of municipal solid waste (In Chinese). Zhejiang University, Hangzhou (PhD).